Continuous Casting Consortium

MechSE

CCC Annual Report 2010

UIUC, August 12, 2010

Transient Turbulent Multiphase Flow and Level Fluctuation Defects in Slab Casting

R. Liu*, J. Sengupta, D. Crosbie**, and B. Thomas***

ArcelorMittal

Department of Mechanical Science & Engineering
University of Illinois at Urbana-Champaign

*****Global R&D at Hamilton***
ArcelorMittal Dofasco Inc.

Continuous Casting Consortium

OUTLINE

- **Modeling SEN flow rate using two models: stopper-based model and level-based model, to provide inlet boundary conditions for the transient simulations**
- **Multiphase Flow Computational Model Validation iva comparison with water model measured data**
- **Turbulent multiphase flow simulation of steel flow in SEN and mold in No. 1 CC caster of Dofasco, using RANS and LES models**
- **Future work**

-- 1st PART: model development for SEN flow rate calculation

Modeling SEN Flow Rate – Objectives

- **to provide accurate inlet boundary conditions for the CFD transient simulations, since:**
  - **SEN flow rate cannot be accurately measured, especially for cases with sudden changes of the stopper rod position, thus needs modeling;**
  - **SEN flow rate change with time as inlet boundary condition is crucial to the accuracy of the transient CFD simulations**

- **to study clogging during casting process**
  - **since clogging cannot be measured directly, but is critical to the flow patterns in the mold and the quality of the final products**
  - **by comparing flow rates from zero-clogging model prediction with the plant trial measurements**

Two Models to Predict SEN Flow Rate

- **Stopper-based Model**
  - **using stopper-rod position to predict the flow rate in SEN**
  - **based on the analysis of Bernoulli's equation**
  - **parameters including:**
    - **measured stopper rod position**
    - **stopper rod zero-flow position**
    - **tundish fraction**
- **Level-based Model**
  - **using measured mold level signal and casting speed to predict the flow rate in SEN**
  - **based on the mass balance at SEN inlet, mold bottom and mold level**
  - **parameters including:**
    - **measured mold level**
    - **measured casting speed**

Sketch of the Stopper Rod System

-- definition of Stopper Rod Opening

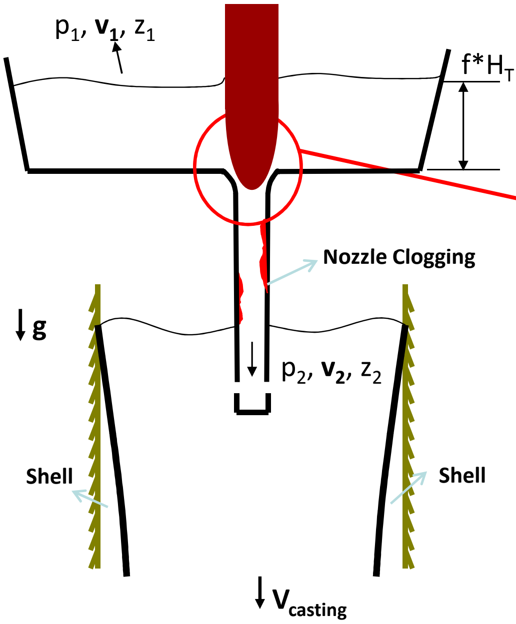

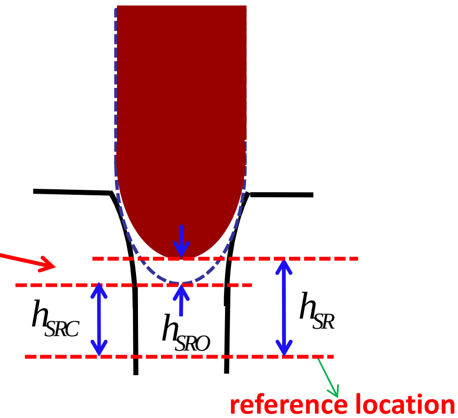

h_{SR} : Stopper Rod Position

h_{SRC} : Stopper Rod Zero-Flow Position (closed position)

h_{SRO} : Stopper Rod Opening

$$h_{SRO} = h_{SR} - h_{SRC}$$

Stopper-based SEN Flow Rate Model

-- Analysis of Bernoulli's Equation

Bernoulli's Equation: **NOTE: Minor loss at SEN port exit is ignored in the model**

$$\frac{p_1}{\rho g} + z_1 + \frac{V_1^2}{2g} = \frac{p_2}{\rho g} + z_2 + \frac{V_2^2}{2g} + h_{minor} + h_{friction} + h_{clogging}$$

At location 1 at tundish meniscus: $p_1 = 1$ atm; $V_1 = 0$ m/s;

At location 2 at port exit: $p_2 = 1\text{atm} \quad + \rho g h_{sen\_sub}$ $V_2 = V_{SEN}$

$$\frac{p_1 - p_2}{\rho g} + z_1 - z_2 = \frac{V_{SEN}^2}{2g} + h_{minor} + h_{friction} + h_{clogging}$$

$$-h_{sen\_sub} + f_{tundish} h_{tundish} + L_{sen} = \frac{V_{SEN}^2}{2g} + h_{minor} + h_{friction} + h_{clogging}$$

Variables in the EQN	Physical Meaning
h_{sen_sub}	SEN submergence depth
$f_{tundish}$	Tundish (weight) fraction
$h_{tundish}$	Total height of the tundish
L_{sen}	Distance from tundish bottom to SEN port center

Stopper-based SEN Flow Rate Model

– Three Sub-models for $h_{friction}$, h_{minor} and $h_{clogging}$

Bernoulli's Equation gives:

$$\frac{V_{SEN}^2}{2g} + h_{minor} + h_{friction} + h_{clogging} = \left(L_{SEN} - h_{SEN\_sub} + f_{tundish} h_{tundish}\right)$$

sub-model 2 (h_{minor}) **sub-model 1** ($h_{friction}$) **sub-model 3** ($h_{clogging}$)

Sub-model 1 for friction head loss:

$$h_{friction} = \xi_1 \frac{V_{SEN}^2}{2g}$$

ξ_1 : function of *Re* number, and SEN surface roughness, SEN diameter and SEN length

Sub-model 2 for Stopper Rod Gap Head loss:

$$h_{gap} = \xi_2 \frac{V_{SEN}^2}{2g}$$

ξ_2 : function of stopper rod opening, SEN inner corss-section area

Sub-model 3 for Stopper Rod Gap Head loss:

$$h_{clogging} = \xi_3 \frac{V_{SEN}^2}{2g}$$

ξ_3 : can only be estimated by comparing predicted SEN flow rate with estimated SEN flow rate from plant trials

Sub-Model 1 – Modeling Friction Head Loss

Original Bernoulli's equation:

$$\frac{V_{SEN}^2}{2g} + h_{gap} + h_{friction} + h_{clogging} = -h_{sen\_sub} + f_{tundish} h_{tundish} + L_{SEN}$$

The friction head loss along the nozzle is modeled as:

$$h_{friction} = C_1 \frac{L_{SEN}}{D_{SEN}} \frac{V_{SEN}^2}{2g}$$

C_1 is a function of *Re* if SEN length and diameter are fixed

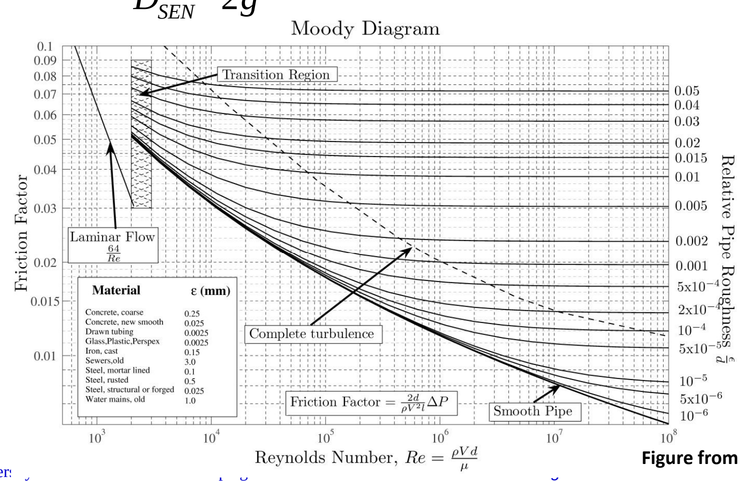

Since:

1.
Flow in the SEN usually reaches the *Re* of 10^5;

2.
The SEN inner surface is not smooth (due to attachment of the alumina oxide inclusions)

$$C_1 = 0.07 \sim 0.08$$

Figure from S Beck and R Collins, University of Sheffield

Sub-Model 2 – Modeling Stopper Rod Gap Minor Loss

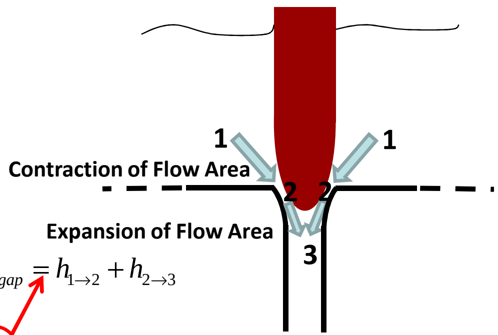

$$h_{gap} = h_{1\to2} + h_{2\to3}$$

$$\frac{V_{SEN}^2}{2g} + h_{\text{gap}} + h_{\text{friction}} + h_{\text{clogging}} = -h_{\text{sen\_sub}} + f_{\text{tundish}} h_{\text{tundish}} + L_{\text{SEN}}$$

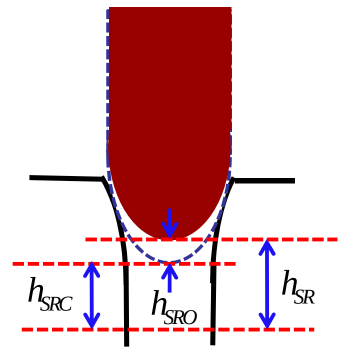

Assume: $A_2 = C_2 h_{SRO}^2$

Minor Loss in Contraction Case (reference [1]), from location 1 to location 2:

$$h_{1\to2} = \xi_{1\to2}\frac{V_2^{\,2}}{2g} \qquad \frac{A_2}{A_1} \to 0 \quad \Rightarrow \quad \xi_{1\to2} = 0.5$$

$$h_{gap} = h_{1\to2} + h_{2\to3} = \frac{V_{SEN}^2}{2g}\left[0.5\left(\frac{A_{SEN}}{C_2 h_{SRO}^2}\right)^2 + \left(\frac{A_{SEN}}{C_2 h_{SRO}^2} - 1\right)^2\right]$$

Minor Loss in Expansion Case (reference [1]), from location 2 to location 3:

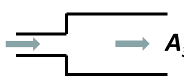

$$h_{2\to3} = \xi_{2\to3}\frac{V_3^{\,2}}{2g} \qquad \xi_{2\to3} = \left(\frac{A_3}{A_2} - 1\right)^2$$

Reference [1]:
Z. Zhang, G. Cui. Fluid Mechanics. Tsinghua University. 2005. ISBN: 7-302-03168-1/O201. pp330.

Final Form of SEN Flow Rate Q_{SEN} from Stopper-based Model

According to the friction head loss and loss models:

$$\frac{V_{SEN}^2}{2g} + h_{\text{gap}} + h_{\text{friction}} + h_{\text{clogging}} = -h_{\text{sen\_sub}} + f_{\text{tundish}} h_{\text{tundish}} + L_{\text{SEN}}$$

$$\frac{V_{SEN}^2}{2g}\left\{1 + 0.5\left(\frac{A_{SEN}}{C_2 h_{SRO}^2}\right)^2 + \left(\frac{A_{SEN}}{C_2 h_{SRO}^2} - 1\right)^2 + C_1\frac{L_{SEN}}{D_{SEN}}\right\} + h_{\text{clogging}} = -h_{\text{sen\_sub}} + f_{\text{tundish}} h_{\text{tundish}} + L_{\text{SEN}}$$

Let $h_{\text{clogging}} = C_3 \dfrac{V_{SEN}^2}{2g}$

$$\frac{V_{SEN}^2}{2g}\left\{1 + 0.5\left(\frac{A_{SEN}}{C_2 h_{SRO}^2}\right)^2 + \left(\frac{A_{SEN}}{C_2 h_{SRO}^2} - 1\right)^2 + C_1\frac{L_{SEN}}{D_{SEN}} + C_3\right\} = -h_{\text{sen\_sub}} + f_{\text{tundish}} h_{\text{tundish}} + L_{\text{SEN}}$$

$$V_{SEN} = \sqrt{\frac{2g\left(-h_{\text{sen\_sub}} + f_{\text{tundish}} h_{\text{tundish}} + L_{\text{SEN}}\right)}{1 + 0.5\left(\frac{A_{SEN}}{C_2 h_{SRO}^2}\right)^2 + \left(\frac{A_{SEN}}{C_2 h_{SRO}^2} - 1\right)^2 + C_1\frac{L_{SEN}}{D_{SEN}} + C_3}}$$

The model consists of three parameters,
C_1 for friction loss along the nozzle
C_2 for minor loss at stopper rod gap
C_3 for head loss due to clogging in the SEN

$$Q_{SEN} = A_{SEN}\sqrt{\frac{2g\left(-h_{\text{sen\_sub}} + f_{\text{tundish}} h_{\text{tundish}} + L_{\text{SEN}}\right)}{1 + 0.5\left(\frac{A_{SEN}}{C_2 h_{SRO}^2}\right)^2 + \left(\frac{A_{SEN}}{C_2 h_{SRO}^2} - 1\right)^2 + C_1\frac{L_{SEN}}{D_{SEN}} + C_3}}$$

Model Parameters Calibration –1

In the final model, the parameters include C_1, C_2, and C_3:

$$Q_{SEN} = A_{SEN}\sqrt{\frac{2g\left(-h_{\text{sen\_sub}} + f_{\text{tundish}}h_{\text{tundish}} + L_{\text{SEN}}\right)}{1+0.5\left(\frac{A_{SEN}}{C_2 h_{SRO}^2}\right)^2 + \left(\frac{A_{SEN}}{C_2 h_{SRO}^2} - 1\right)^2 + C_1\frac{L_{SEN}}{D_{SEN}} + C_3}}$$

1.

As mentioned previously, according to Moody's chart, $C_1 = 0.07 \sim 0.08$

2.

C_2 can be calibrated using the measured Throughput vs. Stopper Rod Opening data, as shown in latter slides;

3. No Clogging Assumption

C_3 is assumed to be zero for the data used to calibrate the parameters (provided by Dofasco);

Variables	Definition and Value	Variables	Definition and Value
h_{sen_sub}	SEN submergence depth (e.g. **0.166** m)	L_{sen}	Length from tudish bottom to SEN port upper edge: (e.g. **1.159** m)
$f_{tundish}$	Tundish (weight) fraction **0~1** (e.g. 0.8)	D_{SEN}	SEN inner diameter (e.g. **0.075** m)
$h_{tundish}$	Total height of the tundish (e.g. **1.451** m)	A_{SEN}	SEN inner cross-section area (e.g. **0.0044** m²)

Model Parameters Calibration –2

Since the tundish fraction influences the pressure head in the system, in order to calibrate the model using the measured data, an estimation of the tundish fraction is needed:

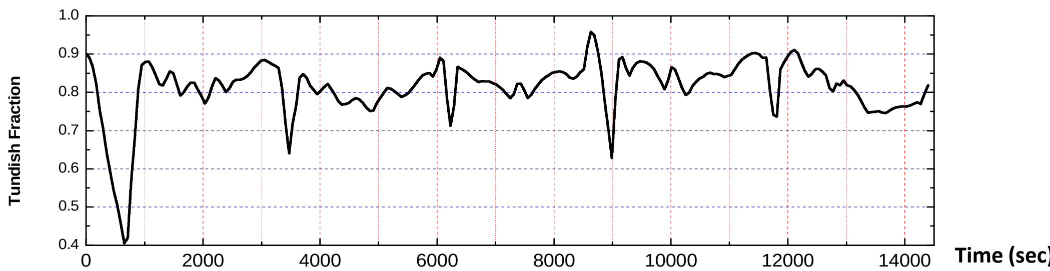

During the process, it is observed that the average tundish fraction stays around 0.8, the calibration will take the following parameters:

Variables	Physical Meaning	Value
C_1	Friction Loss Coefficient	**0.075**
C_3	Minor Loss Coefficient due to Clogging	**0**
$f_{tundish}$	Tundish (weight) fraction	**0.8**

Stopper-based Model
Prediction vs. Measured Data-- Effect of C_2

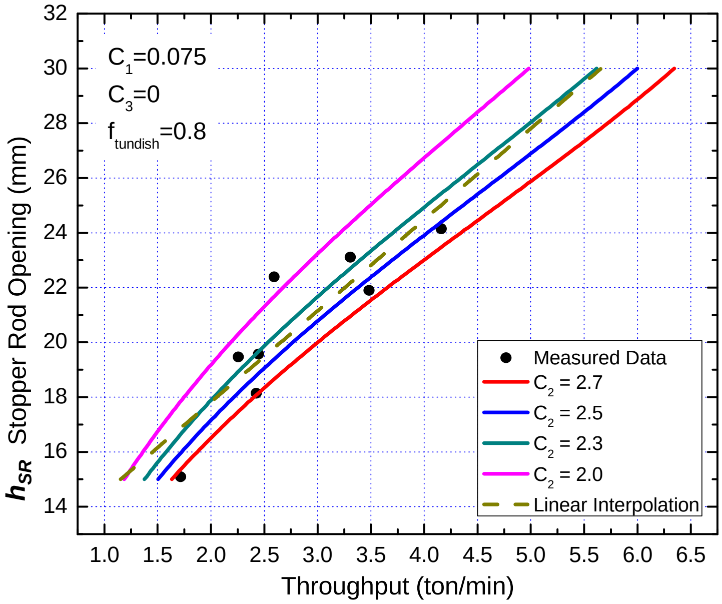

- Increase of the C_2 coefficient leads to an upper-shift of the Stopper Rod Opening vs. Throughput curve; **(shifting curve)**
- Measured data points above the blue curve indicate extra head loss from the measurement (maybe due to clogging)

- **Choose the Stopper Rod gap minor loss coefficient C_2 as 2.7 in following slides**

Influence of Tundish Fraction on SEN Flow Rate

By keeping C_2 at 2.7 and C_1 at 0.075 as mentioned on last slide, varying tundish fraction from 0.2 to 0.8 at an interval of 0.2, the influence of the tundish fraction on the SEN flow rate gives:

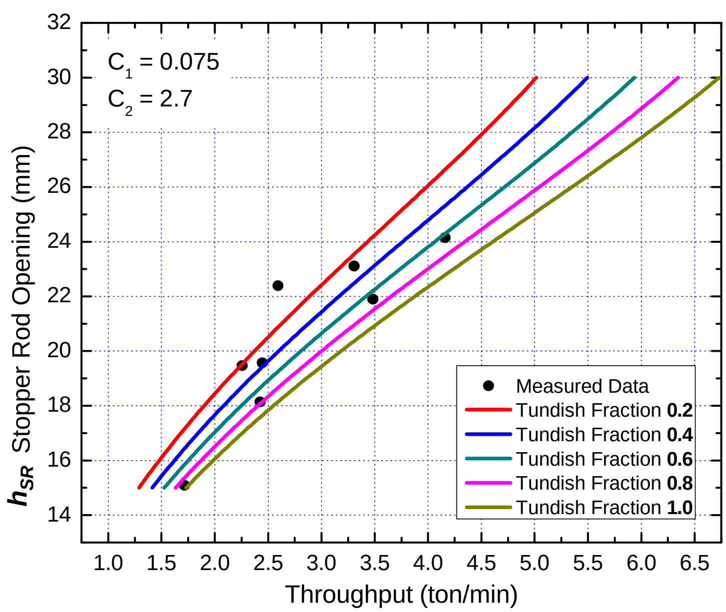

- Increase of the tundish fraction leads to an lower-shift of the Stopper Rod Opening vs. Throughput curve;
- For most processes, the tundish fraction keeps between 0.4~0.8, varying from the blue line to the pink line in the plot **(shifting curve)**

Influence of C_1 on SEN Flow Rate

By keeping C_2 at 2.7 and tundish fraction at 0.8, varying friction factor C_1 from 0.02 to 0.08 at an interval of 0.2, the influence of the friction factor on the SEN flow rate gives:

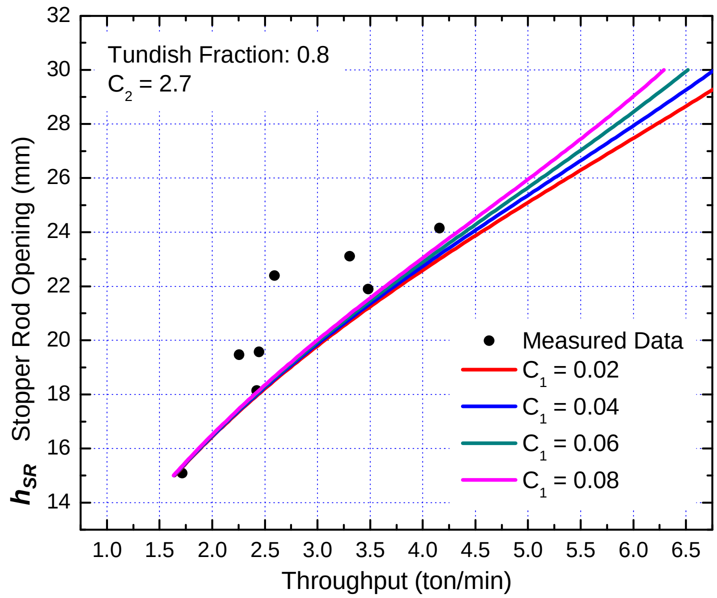

- Little influence is found if the throughput is less than 3.5 ton/min;
- For throughput larger than 3.5 ton/min, increase of the friction factor shifts the stopper rod opening vs. throughput curve upper. (changing curve slope)

Influence of C_3 on SEN Flow Rate

By keeping C_2 at 2.7 and tundish fraction at 0.8, friction factor C_1 at 0.075, the influence of the minor loss coefficient due to clogging on the SEN flow rate gives:

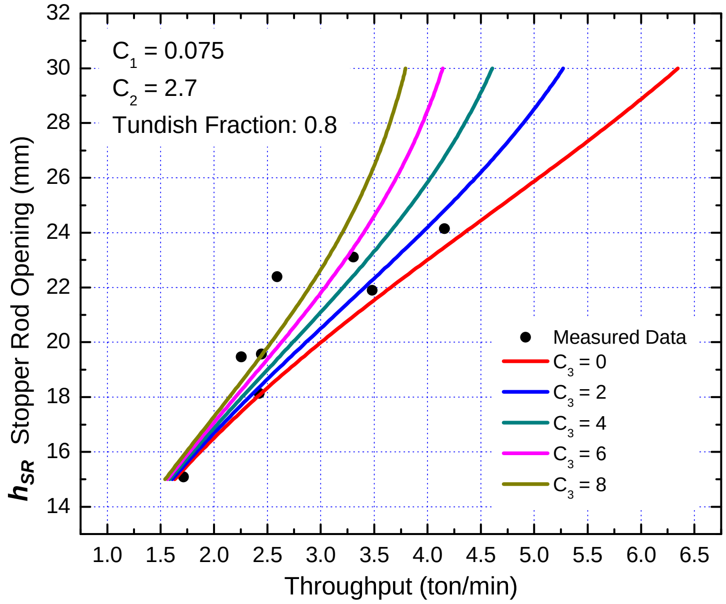

- For throughput larger than 2.5 ton/min, increase of the clogging minor loss coefficient shifts the stopper rod opening vs. throughput curve upper. (changing curve slope)

Level-based SEN Flow Rate Model

Flow rate based on measured casting speed:

$$Q_m(i) = V_{cast}(i) * W * T$$

V_{cast} is casting speed

SEN Flow rate based on mass conservation from the mold-level signal:

$$Q_E(i) = \frac{h_m(i+1) - h_m(i-1)}{2\Delta t}\left(W * T - \frac{\pi d_{SEN,outer}^2}{4}\right) + Q_m(i)$$

h_m is measured mold level

Parameters	Physical Meaning	Parameters	Physical Meaning
h_m	mold level	$d_{SEN,outer}$	outer diameter of SEN
W	mold width	Q_E	SEN flow rate prediction
T	mold thickness	Q_m	Throughput from measured casting speed
Δt	time interval between data points	i	i th time step

Measured Data for Example Transient Case

-- Heat 296078, segments 1~4

measured stopper rod position

measured mold level

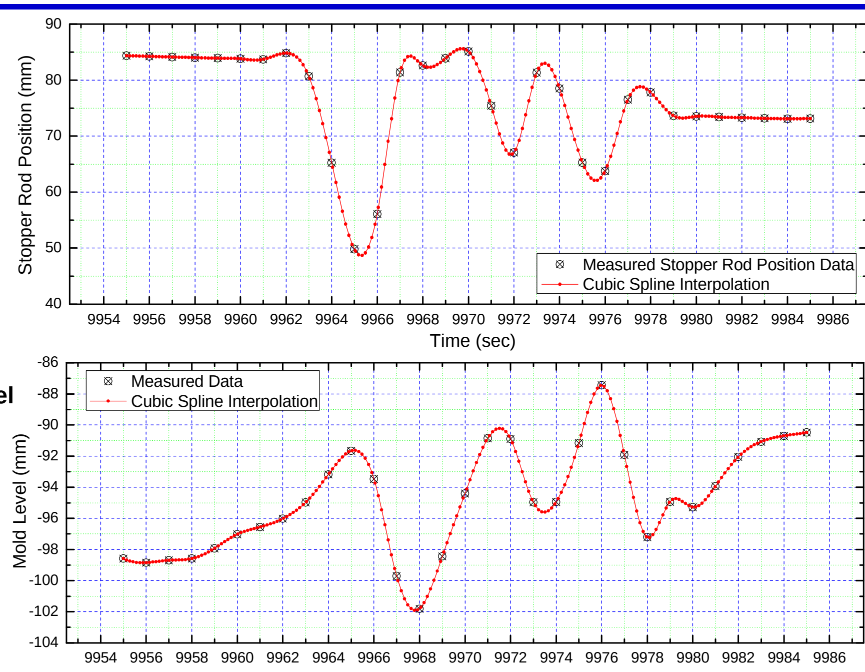

Symbols represent the data recorded by the PI system,

Curves are generated by Cubic Spline Interpolation (to smoothe the data points)

Model Parameters Change during Clog Releasing

C_3 change during "release of clogged material due to bumping"

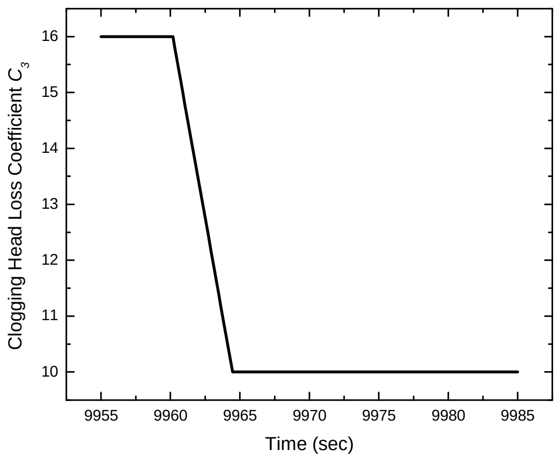

C_2 change

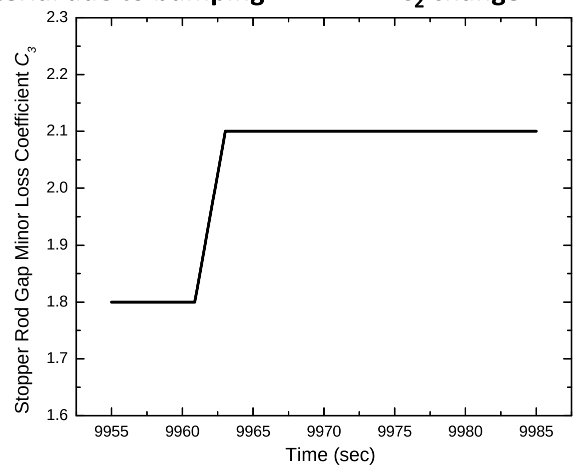

- Sudden reduction of clogging results in a decrease of the clogging head loss coefficient in the model
- Reduction of clogging around stopper-rod tip will increase the stopper rod gap area, thus increase the gap coefficient

Stopper-based vs. Level-based SEN Flow Rate Model -- C_3 decreasing, C_2 increasing, h_{SRC} = 46 mm

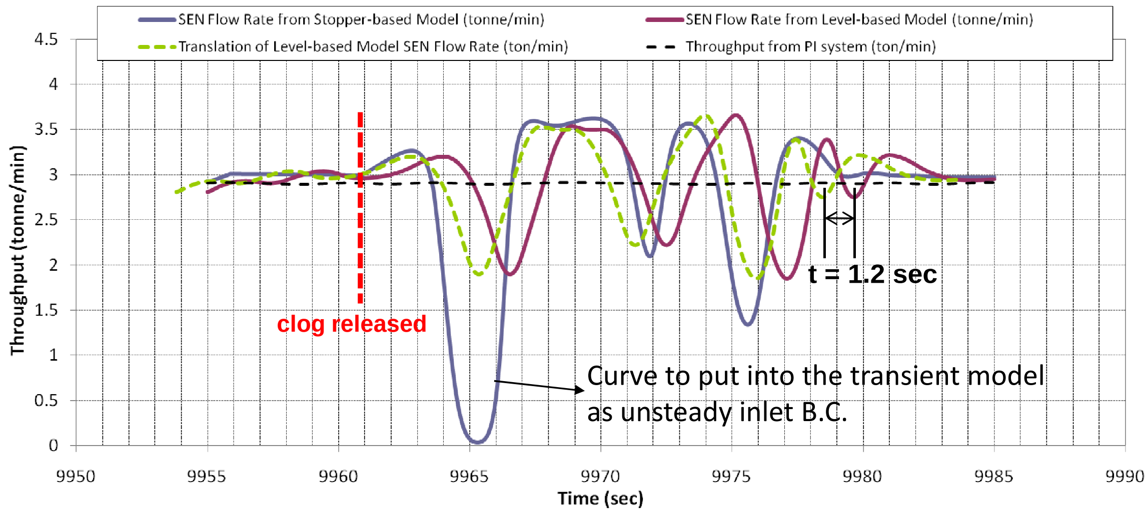

Stopper rod starting position: 46 mm

C_1 = 0.075
C_2 = increasing from 1.8 to 2.2
C_3 : decreasing from 16 to 10

- **"translation of estimated SEN flow rate" curve is translated from the "estimated SEN flow rate" curve by 1.2 sec ahead**
- **1.2 sec is the response time for the meniscus from observation**

Conclusions (for part 1)

- **The model predictions (from stopper-based model) are compared with measurement from Dofasco. Reasonable match is achieved.**
- **Three parameters in the model are calibrated to match with the measured data:**
  - **Friction loss coefficient varies from 0.07~0.08**
  - **Stopper rod gap minor loss coefficient is calibrated between 2.0~2.7**
  - **The clogging minor loss coefficient is assumed 0 in the calibration**

Conclusions (for part 1)

- **Influences of the three coefficients on the SEN flow rate is studied:**
  - **Increase of either the stopper rod gap minor loss coefficient C_2 or the tundish fraction will shift the stopper rod vs. throughput curve lower**
  - **Increase of either the friction loss coefficient C_1 or the clogging loss coefficient C_3 will increase the slope of the curve**
- **This calibrated and validated model can be used to predict clogging in the system by calibrating the clogging minor loss coefficient C_3 according to the measurement**

Model Validation by 1:2.23 Water Model

- **Objective: to validate current computational models with the water model measurement**

water flow rate	4.32 m^3/h
Air gas injection rate	CASE 1: 0 LPM CASE 2: 6.7 LPM (room temperature)
Nozzle submerging depth	76 mm
Nozzle inner diameter	33.6 mm
Mold width	717 mm
Mold thickness	100 mm
Domain width	358.5 mm
Domain thickness	50 mm
Domain length	700 mm
Density (air) Density (water)	1.225 kg/m3 (at velocity inlet) 998.2 kg/m^3
Dynamic viscosity (air) Dynamic viscosity (water)	1.7894e-05 kg/m-s 0.001 kg/m-s
Bubble Diameter (mm)	2.7 mm

Geometry and Mesh for 1:2.23 Water Model

quarter mold

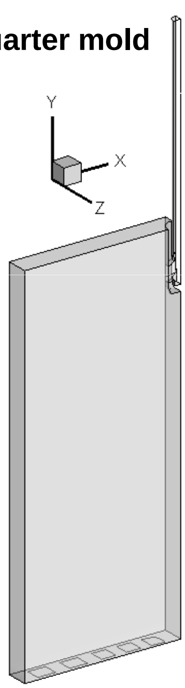

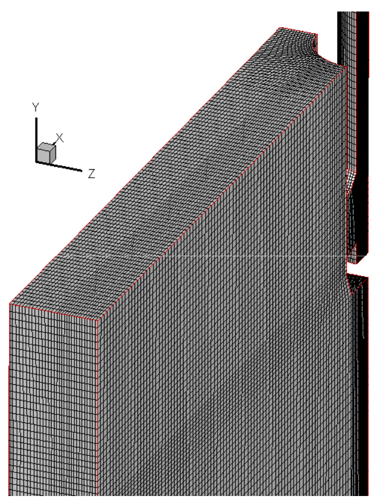

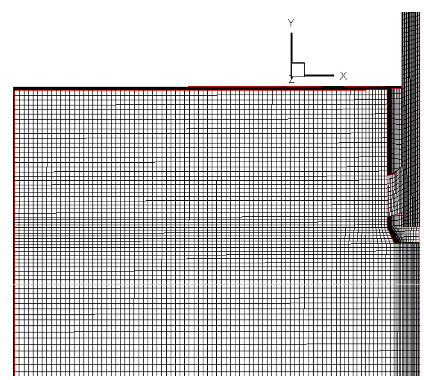

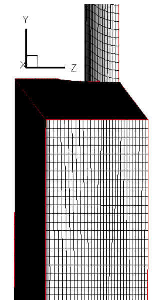

Total:

0.3 million structured hexahedral cells

Computational Details and Boundary Conditions

Computational Details and B.C. Settings:

Models and Schemes	Name
Turbulence Models	k-epsilon with std. wall function
Multiphase Model	Mixture Model
Model for Shell Growth	No
Gas Escaping from Meniscus	Mass Sink for Argon Phase
Advection Discretization	1st order upwinding for k-epsilon model
Pressure Discretization	Body Force Weighted Scheme

Parameters for the transient run:

Time marching scheme	1st order implicit, 0.05 sec time step
Time before collecting statistics	60 sec
Time for the stats	60 sec

Domain Boundaries	B.C.	Domain Boundaries	B.C.
Meniscus	Free-Slip Wall (no slag layer)	Outlet	Pressure Outlet

Single Phase Flow – Water Velocity Distribution

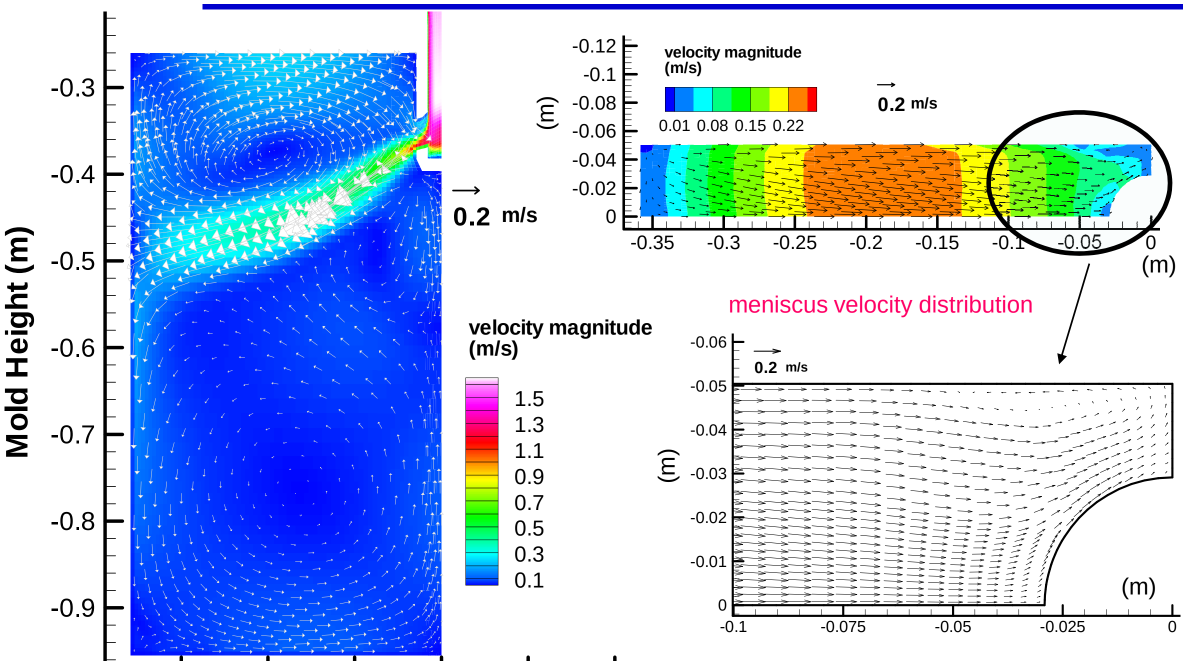

Double Roll Flow Pattern (at center plane between wide faces)

Water Velocity Distribution at SEN Port Exit

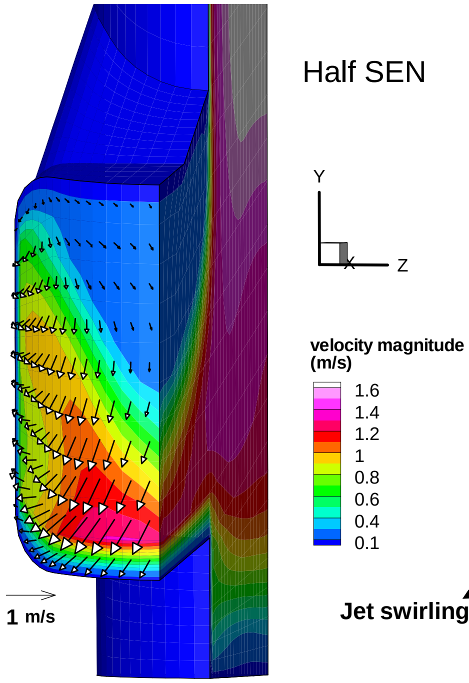

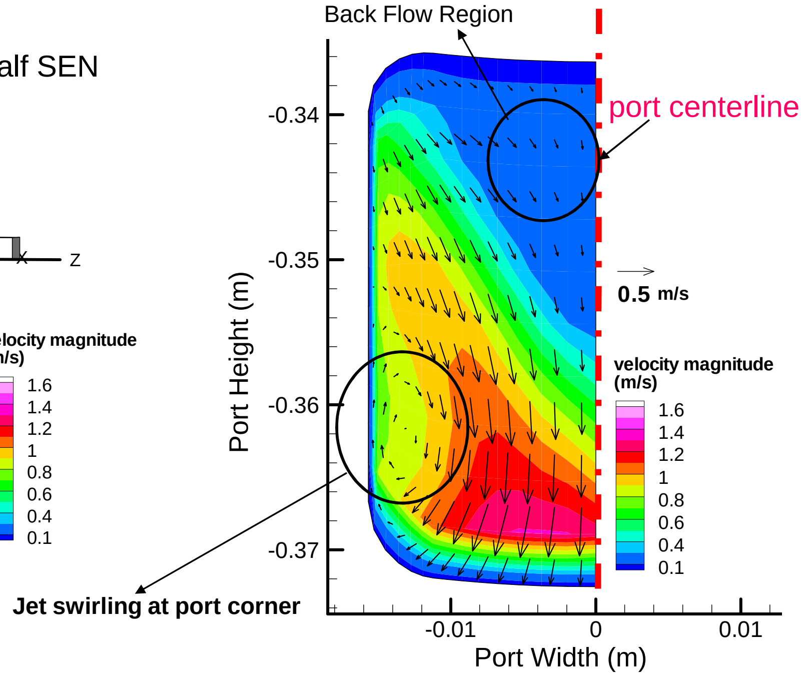

Horizontal Velocity along Meniscus Centerline (Prediction vs. Measurement)

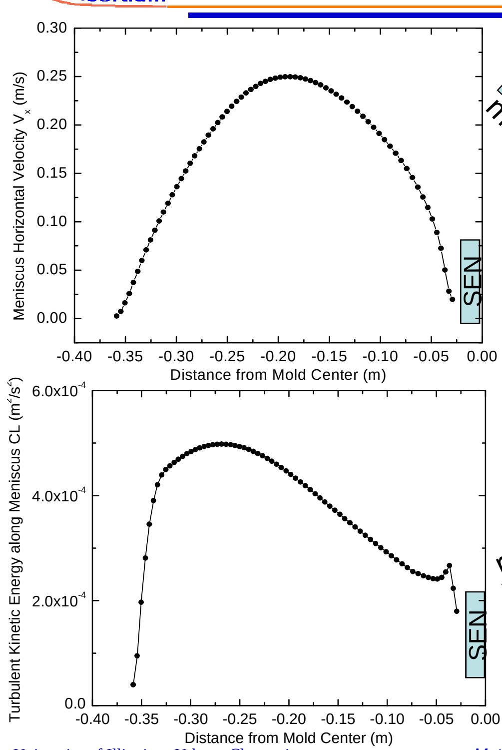

60 sec time-averaged velocity
(RMS of the mean velocity is negligible, 10^{-4} m/s magnitude)

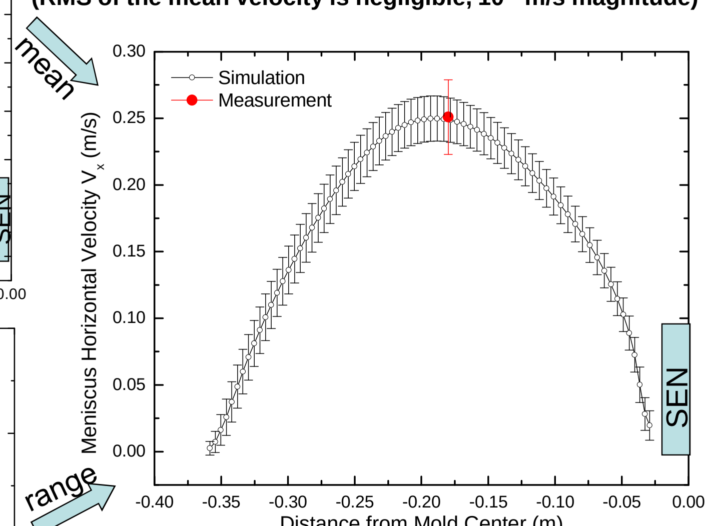

Estimate Fluctuations from calculated turbulent kinetic energy:

$$k = \frac{1}{2}\left(u'^2 + v'^2 + w'^2\right) \Rightarrow |u'| \approx \sqrt{\frac{2}{3}k}$$

Water-Air Two-Phase Flow – Water Velocity Distribution

Continuous Casting Consortium

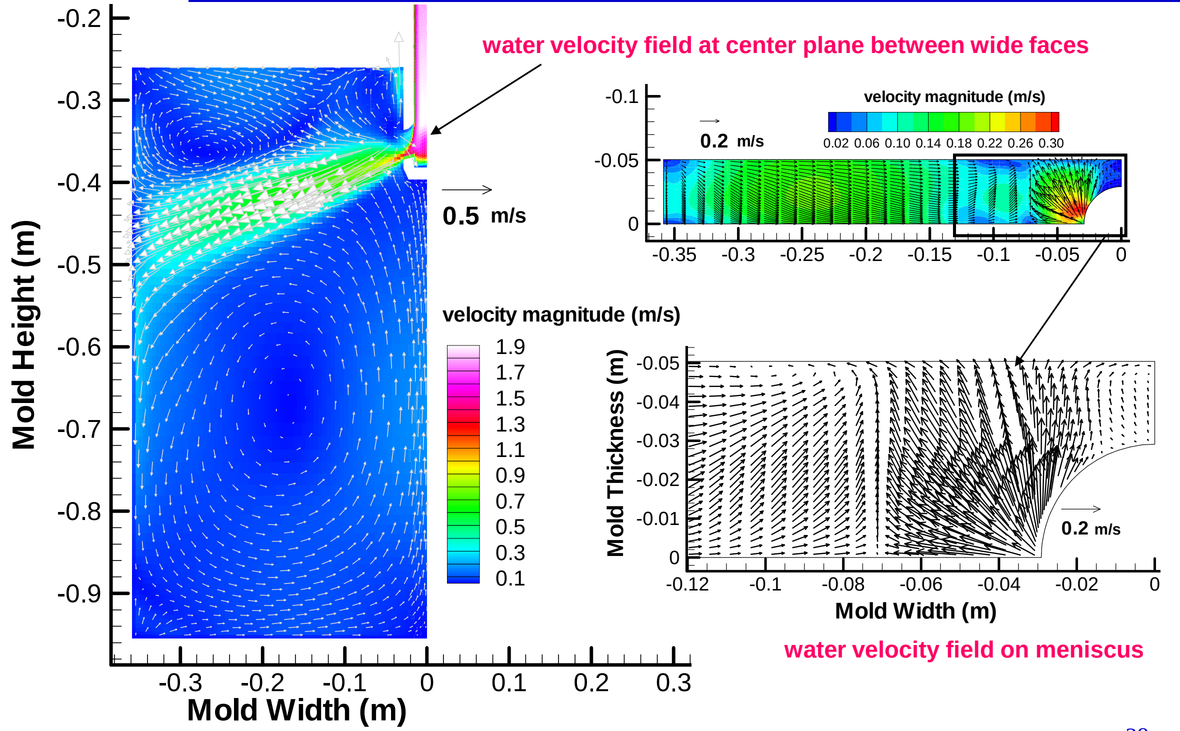

Water Velocity Distribution – at SEN Port Exit

Continuous Casting Consortium

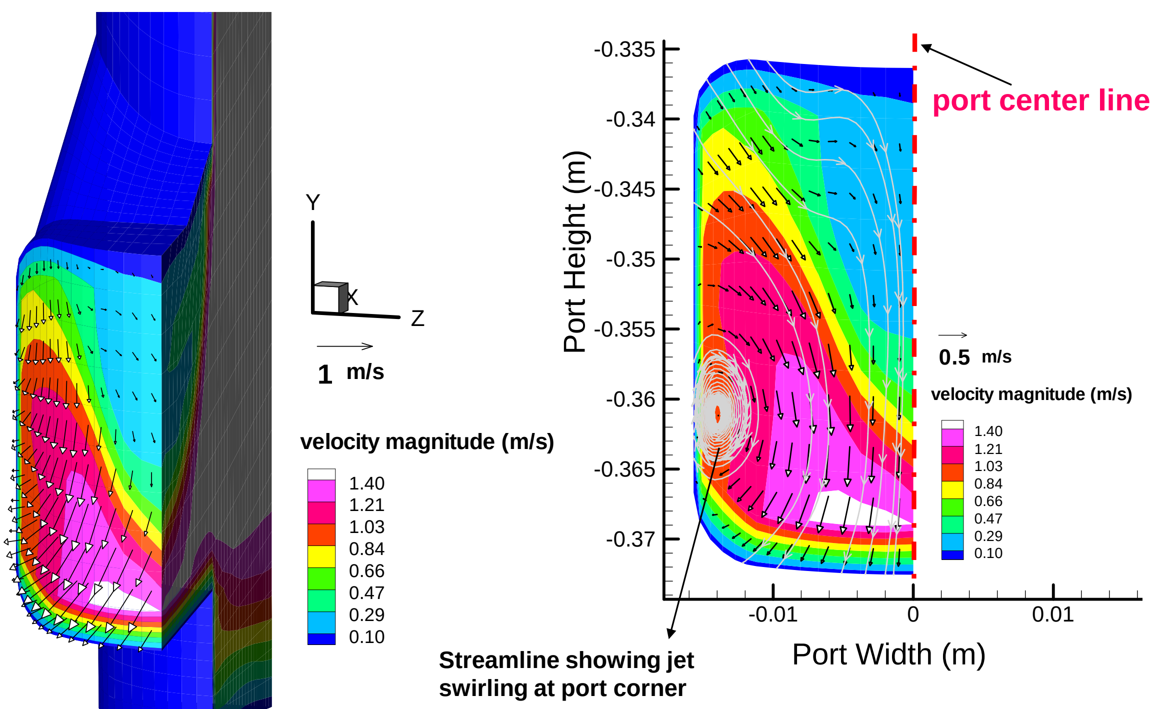

Water-Air Two Phase Flow – Air Velocity Distribution

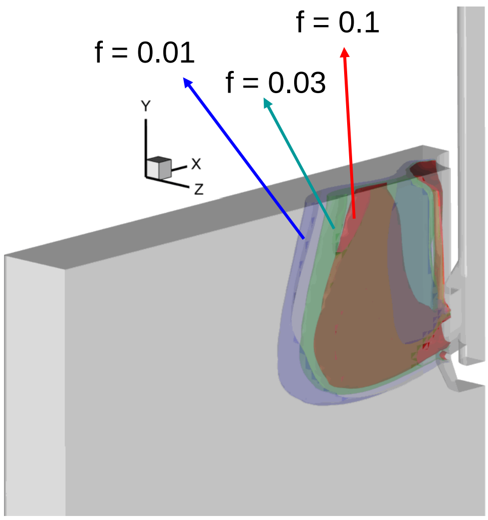

3-D view of air volume fraction Iso-surface

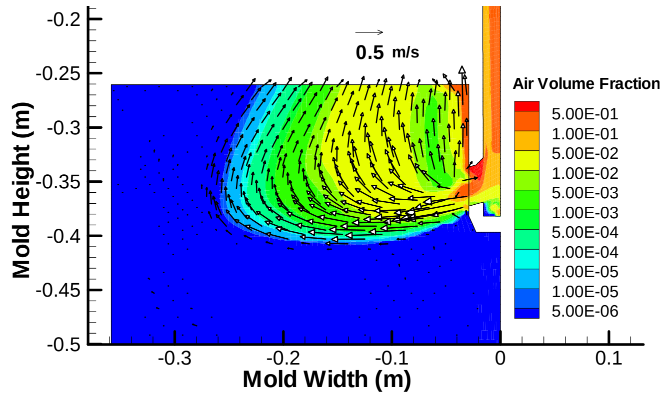

air velocity field on center plane between wide faces

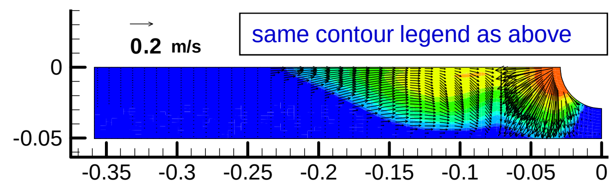

air velocity field on meniscus

Air Velocity Distribution – at SEN Port Exit

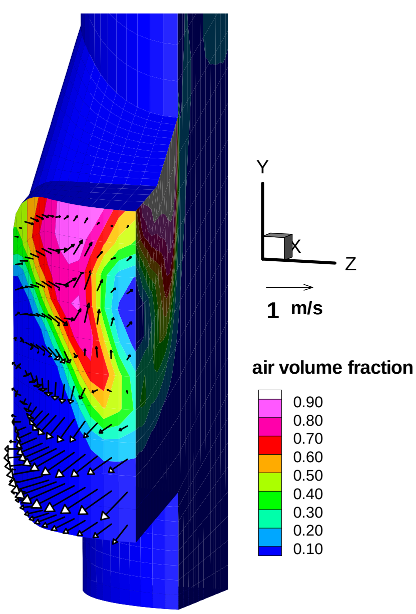

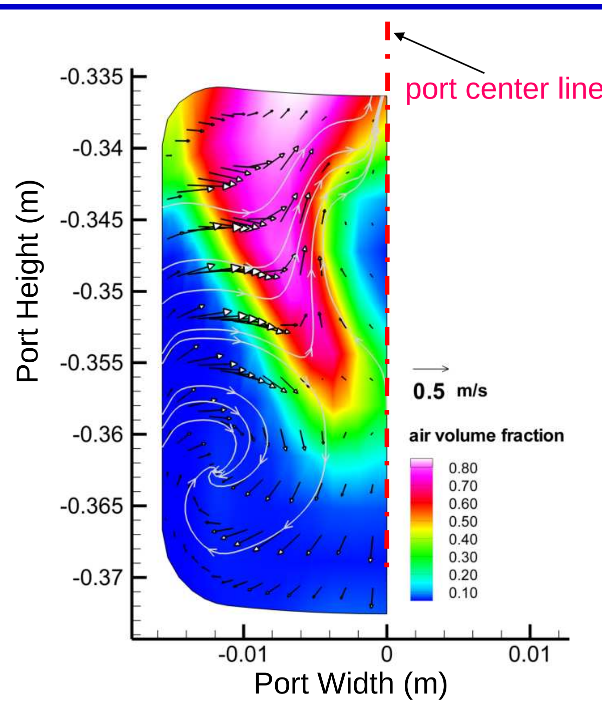

Simulation VS. Measurement – Water Velocity at Meniscus Centerline

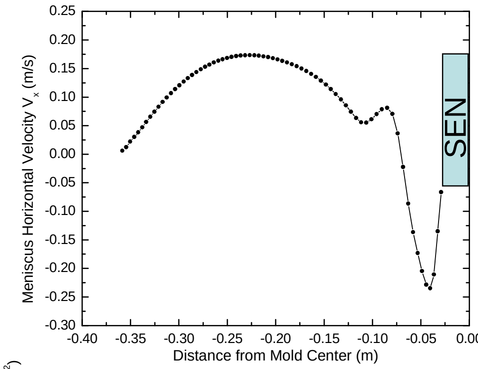

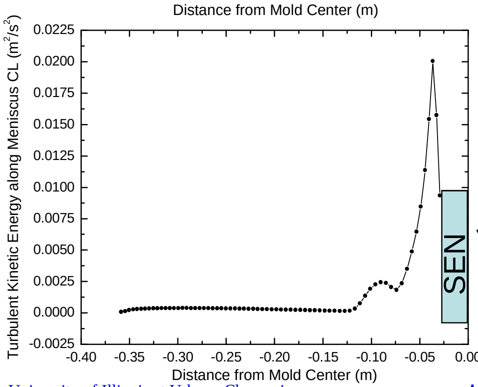

60 sec time-averaged velocity
(RMS of the mean velocity is negligible, 10^{-4} m/s magnitude)

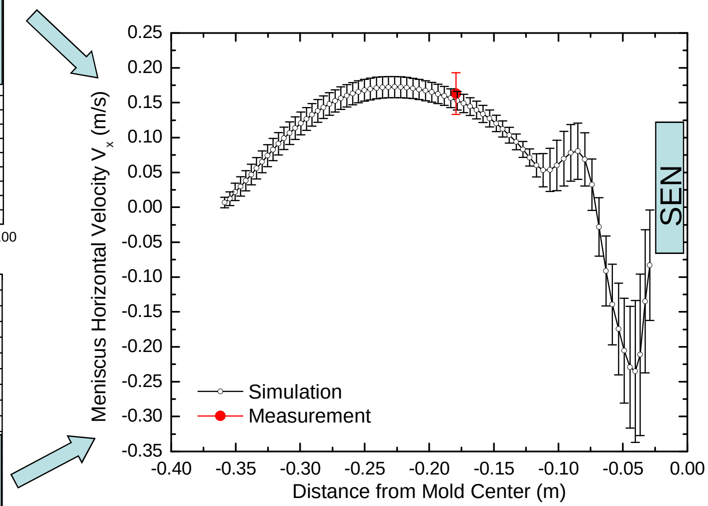

Estimate Fluctuations from calculated turbulent kinetic energy:

$$k = \frac{1}{2}\left(u'^2 + v'^2 + w'^2\right) \Rightarrow |u'| \approx \sqrt{\frac{2}{3}k}$$

Single Phase VS. Multiphase Flow – Water Velocity Distribution

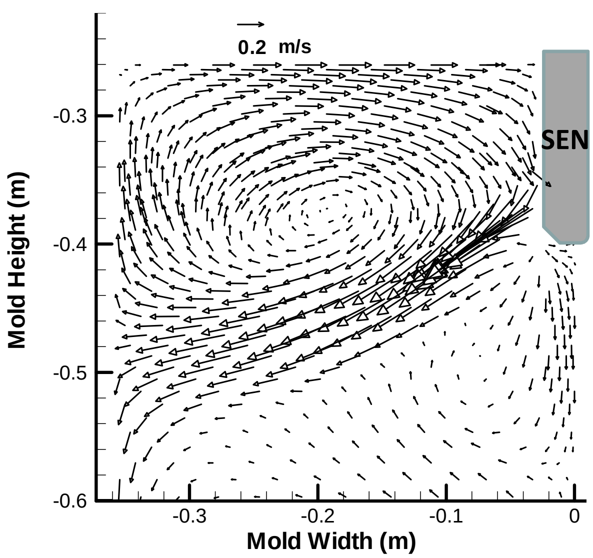

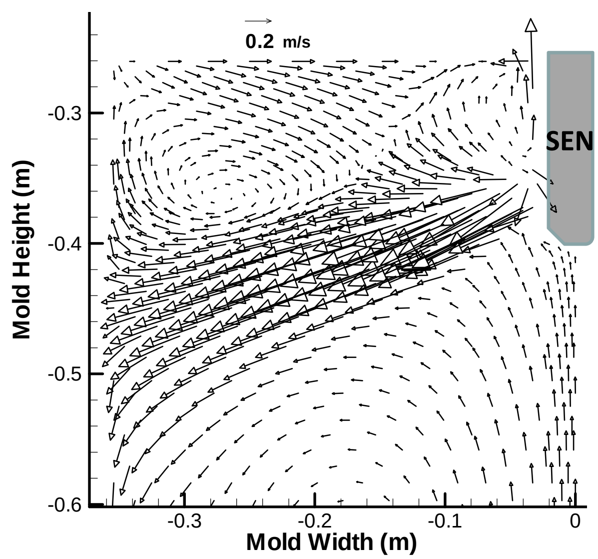

- **Exiting of gas at SEN port exerts a drag force acting on the liquid pointing towards meniscus, which will change the double-roll flow pattern into complex or even single-roll flow pattern, depending on the liquid/gas flow rate, mold width and bubble size distribution.**

Conclusions (for part 2)

- **By comparing simulation results with water model measurements,**
  - **for single phase flow as well as the multiphase flow with relatively low gas volume fraction (8% gas), current model is able to match nicely with experiment data**
  - **gas injection into the mold tends to make more "single-roll" of the flow pattern, depending on the liquid/gas flow rate**
  - **simulation results give lower RMS of velocities than measurements, due to:**
    - **use of URANS (model is diffusive)**
    - **use of 1st order upwinding for advection terms (diffusive scheme)**
    - **use of quarter mold as domain (suppressing the bias flow between left and right part of the mold)**

-- 3rd PART: Computational Model Validation

Simulation of Dofasco No. 1 Steel Caster

-- Heat 296078, Time 9955 sec

Geometry and Mesh:

blocks for structured grid meshing

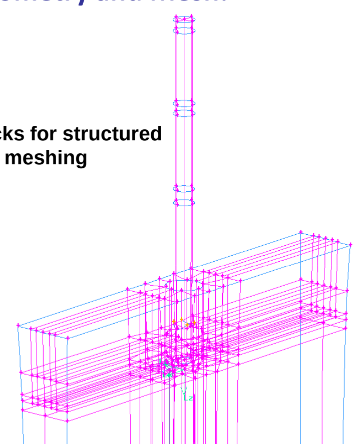

Total Mesh:

800,000 hexahedral cells

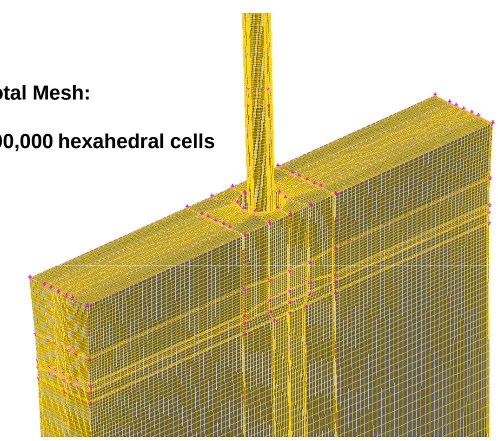

Model Geometry Parameters	Value
Mold Width (m)	**1.472**
Domain Length (m)	**3.0**
Mold Thickness at Meniscus (m)	**0.225**
SEN Outer/Inner Diameter (m)	**0.130/0.075**
SEN Submergence Depth (m)	**0.166**
Solidification Constant for Shell Thickness (in/sqrt(min))	**0.98**

Computational Schemes and Boundary Conditions

Computational Details and B.C. Settings:

Models and Schemes	Name
Turbulence Models	1. k-epsilon with std. wall functions 2. LES with Wale Model
Multiphase Model	Mixture Model
Model for Shell Growth	Mass and Momentum Sinks for Liquid Steel
Gas Escaping from Meniscus	Mass Sink for Argon Phase
Advection Discretization	1. 1^{st} order upwinding for k-epsilon model 2. Bounded Central Diff. for LES
Time Marching Scheme	1. 1^{st} order implicit scheme for k-e model, 0.05 sec time step 2. 2^{nd} order implicit scheme for LES, 0.002 sec time step
Pressure Discretization	Body Force Weighted Scheme

Time before collecting statistics	10 sec
Time for the averaging	20 sec

Domain Boundaries	B.C.	Domain Boundaries	B.C.
Meniscus	No-Slip Wall (with slag layer)	Outlet	Pressure Outlet

Argon Gas Injection and Process Parameters

argon injection at stopper rod tip
1.73 SLPM

argon injection at upper tundish nozzle
4.03 SLPM

plate argon injection
8.02 SLPM

SEN argon injection
1.73 SLPM

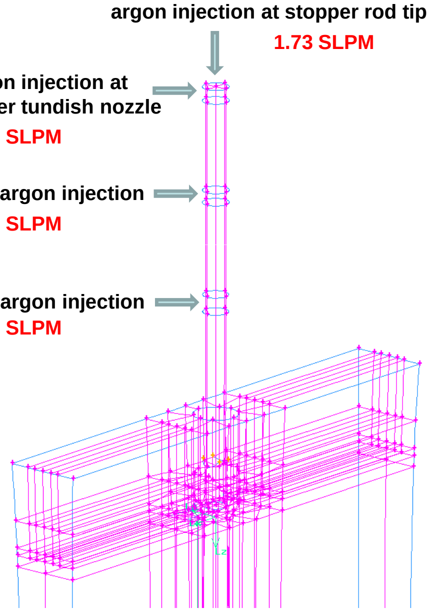

Process Parameters	Values
Casting Speed (m/min)	1.2 m/min
Argon Injection Method	shown on the left

Material Properties	Values
Liquid Steel Density (kg/m3)	7520
Argon Density (kg/m3)	1. At 293 K, 0.55 2. At 1823 K, 0.291
Liquid Steel Dynamic Viscosity (Pa*s)	0.006
Argon Dynamic Viscosity (Pa*s)	1. At 293 K, $2.2816*10^{-5}$ 2. At 1823 K, $8.1825*10^{-5}$
Argon Mean Bubble Dia (mm)	2.5

Liquid Steel Velocity Distribution at Center Plane between Wide Faces – by k-epsilon Model

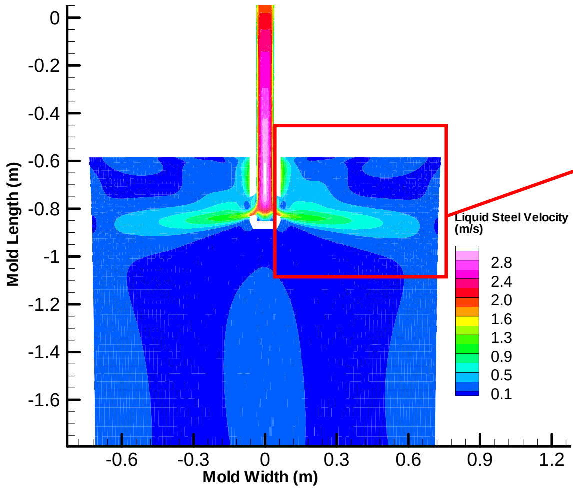

Contour for Liquid Steel Velocity Distribution

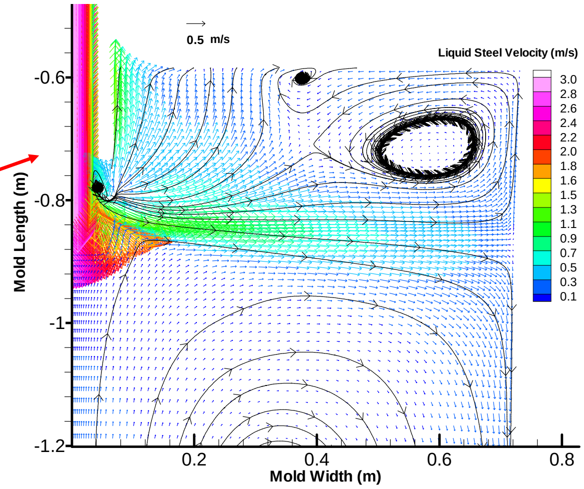

Vector Plot for Liquid Steel Velocity Distribution

- Partial double roll flow pattern is observed (complex flow pattern)
- Jet exiting the port is split into an upward portion heading to meniscus, and a remaining portion impinging the narrow face

Argon Gas Velocity Distribution in the Mold – by k-epsilon with Mixture Model

argon volume fraction distribution at meniscus (same legend as below)

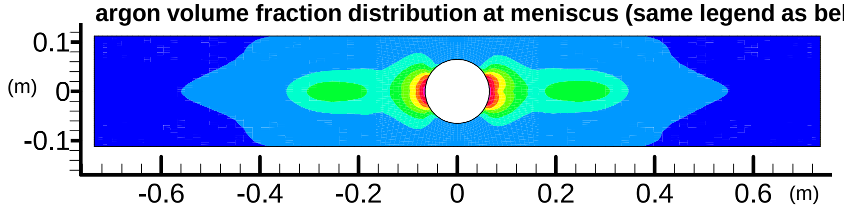

argon volume fraction distribution at center plane between wide faces

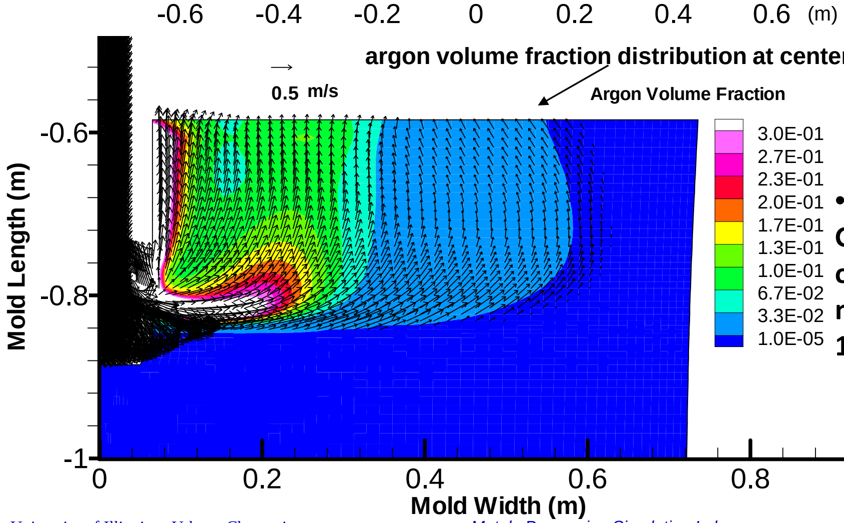

- Gas gathers near the SEN outer surface, with a maximum gas velocity of 1.0~1.2 m/s

Steel/Argon Velocity Distribution at SEN Port Exit – by k-epsilon Model

Time-averaged Liquid Steel Velocity

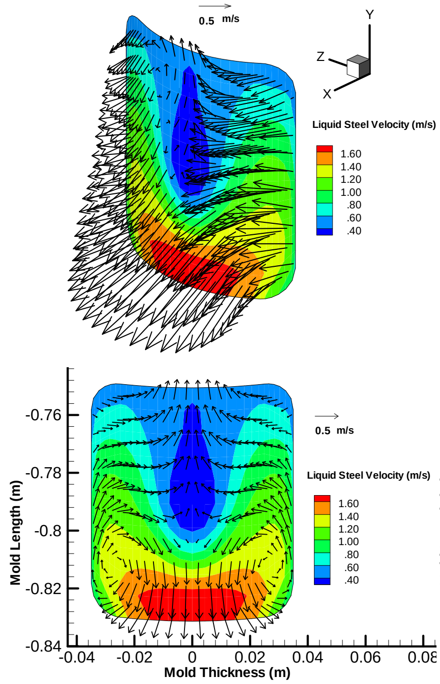

Time-averaged Argon Velocity

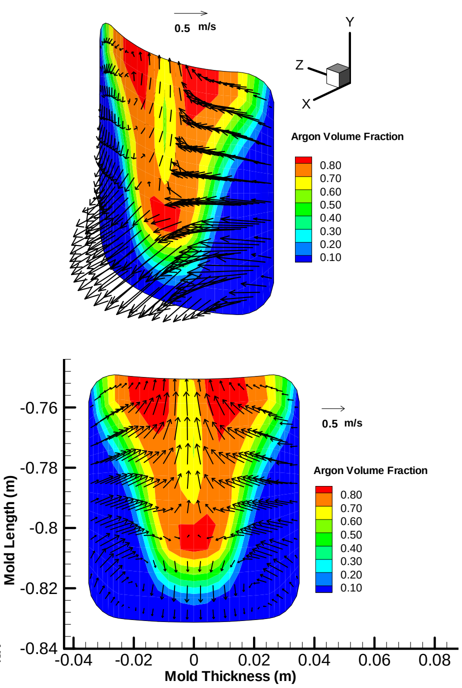

- Jet swirling at port lower corners
- Part of the jet bends towards meniscus due to the gas drag force
- Maximum jet velocity is found at the port bottom
- Gas gathers both near the top edge of the port and in the lower middle part of port
- Gas "jet" is split into two parts, one moving upward to meniscus and the other part moving with the liquid steel jet

Liquid Steel Velocity Distribution at Center Plane between Wide Faces – by LES with Wale Model

Instantaneous Steel Flow Field at Center Plane

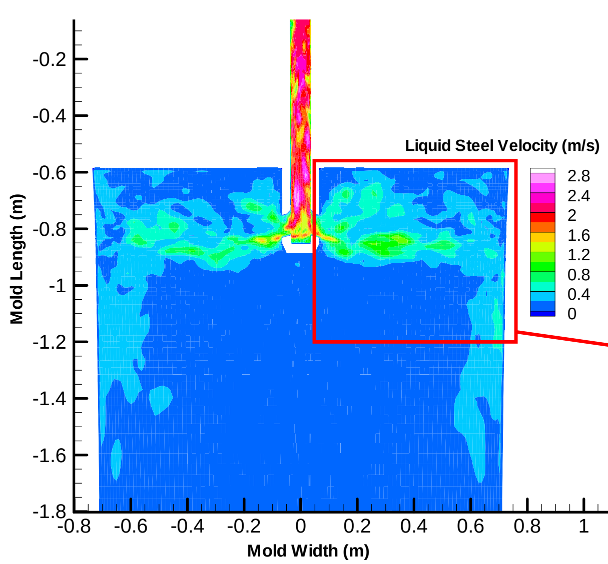

Contour for Instantaneous Liquid Steel Velocity Distribution

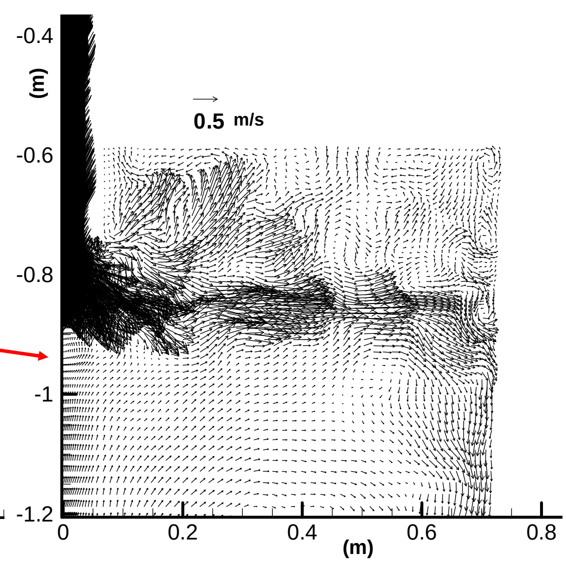

Vector Plot for Instantaneous Liquid Steel Velocity

Argon Gas Velocity Distribution in the Mold – by LES with Wale Model

Instantaneous Argon Flow Field at Center Plane

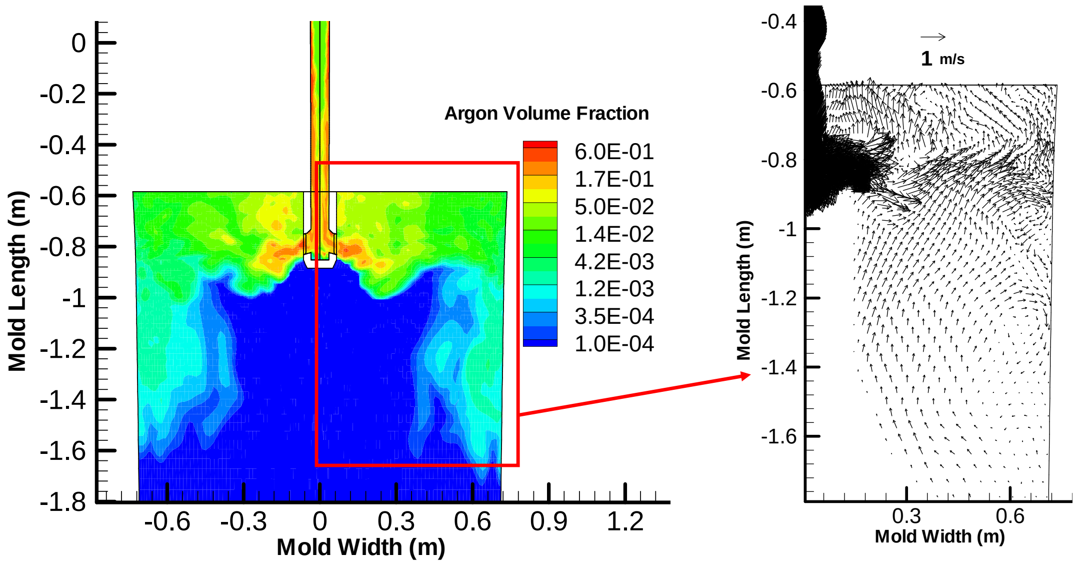

Contour for Instantaneous Argon Gas Velocity Distribution | **Vector Plot for Instantaneous Argon Gas Velocity**

- **Argon gas is dragged further down the mold by liquid steel, and then floats to the mold top surface**

Steel/Argon Velocity Distribution at SEN Port Exit – by LES with Wale Model

Instantaneous Liquid Steel Velocity | **Instantaneous Argon Velocity**

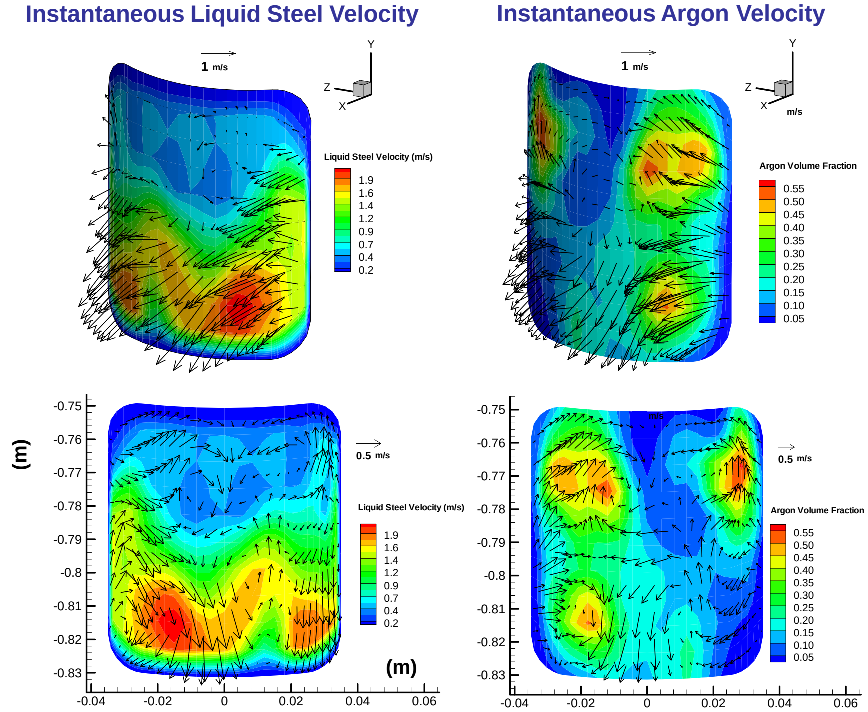

- **Maximum liquid steel velocity is found at the port corner**
- **Velocity field is not symmetric for the left and right part of the port, unlike RANS**
- **Gas gathers both near the top edge of the port and in the lower part of the port**

Mean Argon Gas Volume Fraction Distribution -- RANS VS. LES

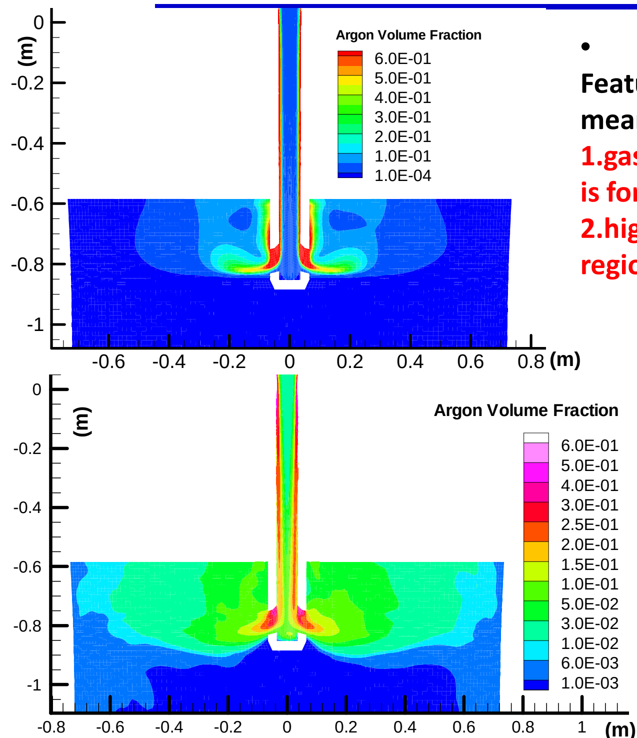

- **Features in Common for RANS and LES mean:**
  1.gas sheet attaching at SEN inner surface is formed
  2.higher gas concentration at the upper region of port exit

- **Difference:**
  1.LES has a gas region spreading to the lower portion of mold, while RANS does not

  2.RANS has higher gas volume fraction at port exit, and the gas sheet in SEN

Time-averaged field over 20 sec

Mean Liquid Steel Velocity Distribution -- LES VS. RANS

Time-averaged Steel Flow Field at Port Exit

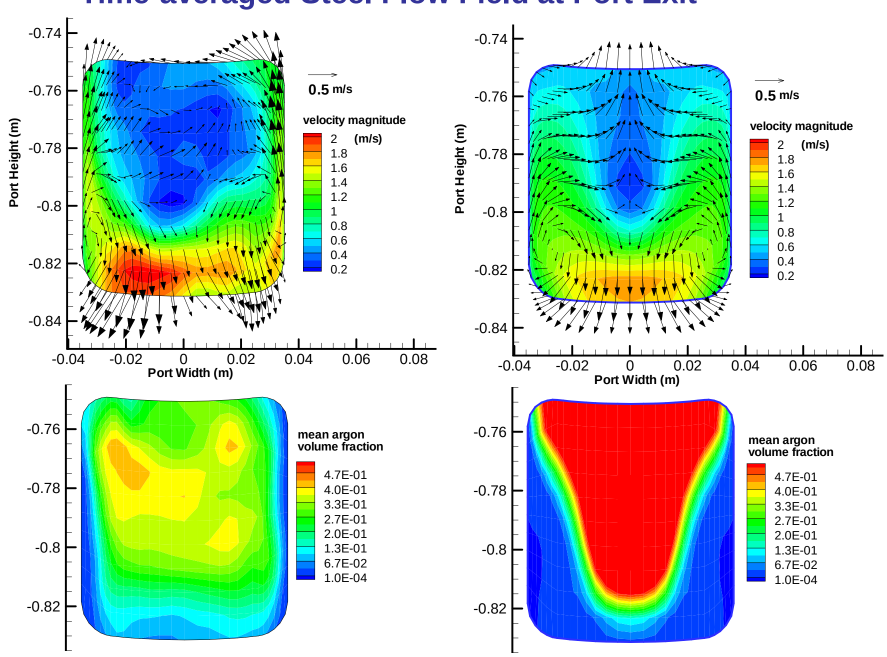

--by LES Wale Model, averaged over 20 sec **--by k-epsilon Model**

- **20 sec is not long enough for the LES port mean velocities to achieve symmetry**
- **major difference observed in gas volume fraction distribution at port exit**

Mean Liquid Steel Velocity Distribution -- LES VS. RANS

Continuous Casting Consortium

Instantaneous Argon Flow Field at Center Plane between Broad Faces

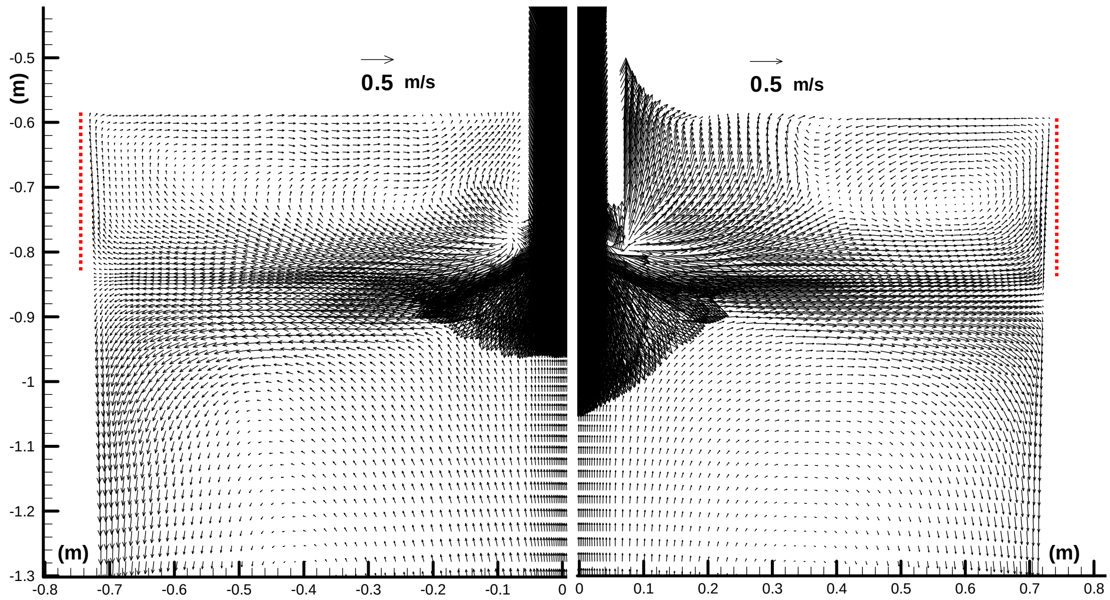

Velocity Distribution by LES Wale Model -- time averaged field over 20 sec

Velocity Distribution by k-epsilon Model

Conclusions (for part 3)

Continuous Casting Consortium

- **By comparing simulation results from LES and URANS, the following features are observed:**
  - **LES shows less gas gathering at upper SEN port exit, thus less drag force for liquid steel;**
  - **LES shows a larger gas region, down the liquid pool;**
  - **Reasonable match between LES mean velocity field (average over 20 sec) and the RANS results is obtained**

- **Due to the difference of the two models in predicting argon gas volume fraction distribution, the flow patterns from LES and URANS are slightly different:**
  - **LES tends to generate double-roll flow patterns, while URANS tends to generate complex flow patterns (especially at high argon injection rate)**

Future Work –1

- **Use URANS to simulate the transient case proposed in previous slides, to find:**
  - **meniscus level based on dynamic pressure from the CFD models**
  - **compare this simulated meniscus level with real measurement to further validate and calibrate the stopper-based model**
  - **the most accurate curve of SEN flow rate vs. time, via this iterative procedure**

- **Carry out LES to study the transient flow behavior during the multiple stopper rod movements during this process, to find out:**
  - **how the flow pattern in the mold is changed by the varying inlet velocity (flow rate)**

Future Work –2

- **Perform particle transport and entrapment simulations during LES run, to find:**
  - **how the particles are entrapped due to the flow pattern change**
  - **preferential locations for the inclusions to get entrapped**

- **Perform this modeling process for different casting conditions, to find the critical stopper rod moving velocity that can cause sliver defects**

Acknowledgment

- Continuous Casting Consortium Members (ABB, ArcelorMittal, Baosteel, Corus, LWB Refractories, Nucor Steel, Nippon Steel, Postech, Posco, ANSYS-Fluent)
- M. Yavuz in ArcelorMittal Global R&D at East Chicago
- Rajneesh and other graduate students and visiting scholars at Metals Processing Simulation Lab, UIUC